On the parameters used in finite element modeling of compound peripheral nerves

Nicole A Pelot[1], Christina E Behrend[1], and Warren M Grill[1,2,3,4]

[1] Duke University
Department of Biomedical Engineering
Room 1427, Fitzpatrick CIEMAS
101 Science Drive
Campus Box 90281
Durham, NC 27708

[2] Duke University, Department of Electrical and Computer Engineering, Durham, NC, USA
[3] Duke University, Department of Neurobiology, Durham, NC, USA
[4] Duke University School of Medicine, Department of Neurosurgery, Durham, NC, USA

Email: warren.grill@duke.edu

Journal of Neural Engineering

Short title: Parameters in neural finite element modeling

Keywords: neural computational modeling; peripheral nerve stimulation; finite element method; neuroengineering; neural engineering; vagus nerve stimulation

Supplement A – Literature Review of Perineurium Representations in Computational Models

Table 4. Compilation of implementations of perineurium in computational models, including sheet resistance, thickness, and resistivity, as applicable. The values that are underlined and italicized were calculated from information in the publication. Implementation methods (A, B, C, D) are described in the text and in Table 2; note that methods A & C produce identical results and methods B & D produce identical results if correctly implemented, but methods A & C produce different results than B & D. Publications that used constant thickness for the perineurium necessarily used both constant sheet resistance and constant resistivity (implementation methods C and D, respectively). R_s: sheet resistance.

Publication	**Implementation method (see Table 2)**	**R_s (Ω-m²)**	**Thickness (µm)**	**Resistivity (Ω-m)**	**Reference/justification for chosen values**
(Weerasuriya et al., 1984)	N/A	0.0478	--	--	Impedance measurements of perineurium from frog sciatic nerve.
(Veltink et al., 1989)	D	--	Could estimate from Fig 2 & 3	100	Perineurial conductivity (0.01 S/m → 100 Ω-m) set to a value lower than their epineurial conductivity (0.1 S/m → 10 Ω-m), which was chosen to be higher than the conductivity of fat (0.04 S/m → 25 Ω-m).
(Meier et al., 1992)	A & B, but assumed A	0.0005	10	50	"The conductance of the epineurium of frog sciatic nerve was measured by Weerasuriya et al. who found σ_s = 2000 S/m² (Weerasuriya et al. 1984)[a]. They did not report the thickness of the epineurium but assuming a value of 10 µm, one calculates a specific resistance of 5000 Ω-m.[b] An epineural sheath with this resistance will almost act as an insulator which is in contrast to the finding of Tasaki who found in his measurements of σ_p [the conductivity of nerve bundle in radial direction] that the resistance of the epineurium could almost be neglected (Tasaki 1964). The present authors used mostly σ_s = 2000 S/m², assuming a sheath thickness of 10 µm and a specific resistance of 50 Ω-m, which is about twice the specific resistance of fat (Geddes and Baker 1967)." [a] This is incorrect. Weerasuriya et al. found a conductance of 20 S/m². [b] See footnote a. Using the correct Weerasuriya value of σ_s = 20 S/m² yields 5000 Ω-m (with thk = 10 µm), as stated here. But in the last sentence of the paragraph, they state that they used 50 Ω-m, which results from their incorrectly stated value of σ_s = 2000 S/m².
(Goodall et al., 1995)	C & D, but assumed C	<u>*0.0149*</u>	50	298	"T. Frieswijk, personal communication (calculated from Weerasuriya 1989 [sic]). In the model, a perineurium thickness of 50 µm was used. This was equivalent to a 35 µm perineurium with a conductivity of 0.0026 S/m [385 Ω-m]."
(Koole et al., 1997)	D (& maybe C)	--	Could estimate from Fig 2	1190 (?)	"The conductivity of the perineurium was derived from Weerasuriya et al. (Weerasuriya et al. 1984), assuming a 40 µm thickness of the perineurium in their experiments. It has been suggested that the thickness of the perineurium roughly equals 5% of the diameter of a fascicle (Sunderland 1978, p. 41). The thickness of the modeled perineurium was too large in comparison with the diameters of the fascicles. Therefore, the conductivity of the perineurium, perpendicular to its surface, was increased by a correction factor. The conductivity of the perineurium, parallel to its surface, was reduced by the same factor." Their implementation of the correction factor was unclear, especially since a single conductivity value was provided for the perineurium (i.e. modeled as isotropic tissue).
(Struijk, 1997)	C & D	<u>*0.0149*</u>	50	294	Goodall 1995 (Goodall et al., 1995)
(Frieswijk et al., 1998)	A?	0.011			"The perineurium sheath impedance as of frog sciatic nerve is presented, in the form of an impedance locus, by Weerasuriya et al. (1984). It has a DC value of 20 S/m² and an absolute value of 45 S/m² at 10 kHz. The latter value is best suited for our model, as our stimulus is a 100 µs duration rectangular pulse, but it has to be corrected to account for the temperature difference between frog and rat, as follows: Whereas Weerasuriya et al. (1984) took measurements at a temperature of 21ºC the body temperature in the rat is 37ºC. By scaling with the Q_{10} factor one can account for this difference: $\sigma_s(37^oC) = \sigma_s(21^oC) * Q_{10}^{(37-21)/10}$ Bostock (1983) presents Q_{10} = 1.5, yielding an increase to σ_s = 90 S/m²."
(Deurloo et al., 1998)	C & D	<u>*0.0149*</u>	50	298	Frieswijk 1998 (Frieswijk et al., 1998)
(Perez-Orive and Durand, 2000)	C & D	<u>*0.0398*</u>	25	1592	No ref
(Rahal et al., 2000)	C & D	<u>*0.0149*</u>	50	294	Struijk 1997 (Struijk, 1997)

(Choi et al., 2001)	C & D, but assumed D	*0.0143*	30	478	"The perineurium resistance was obtained from frog experiments (Weerasuriya 1984) with the assumption that the perineurium thickness in those experiments was 100 µm." Note that the Weerasuriya perineurium thickness was assumed to be 100 µm, but then the perineurium was modeled with a thickness of 30 µm.
(Deurloo et al., 2003)	C & D	*0.0149*	50	298	Deurloo 1998 (Deurloo et al., 1998) "Although the thickness of the perineurium roughly equals 5% of the diameter of the fascicle (Sunderland 1978), the perineurium layers of all fascicles were given a thickness of 50 µm, according to the minimum grid size in the model."
(Hennings et al., 2005)	C & D	*0.0149*	50	294	Vučković 2003 (2005?) (Vučković et al., 2005)
(Vučković et al., 2005)	C & D	*0.0149*	50	294	No ref
(Yoo and Durand, 2005)	C & D	*0.0238*	50	476	Choi 2001 (Choi et al., 2001)
(Grinberg et al., 2008)	D	--	From data: 3%*d_{fasc} Also evaluated: 0, 3, 15, 30, 50 µm 0 to 15%*d_{fasc}	476 Also evaluated 0.5 to 5000	Evaluated activation thresholds in response to different perineurium thicknesses and conductivities. Sunderland 1978 (Sunderland and Bradley, 1952) Choi 2001 (Choi et al., 2001) Other references listed for range of conductivities.
(Schiefer et al., 2008)	D	--	3%*d_{fasc}	500	Grinberg 2008 (Grinberg et al., 2008) Choi 2001 (Choi et al., 2001)
(Kent and Grill, 2013)	D	--	3%*d_{fasc}	1205	Grinberg 2008 (Grinberg et al., 2008) Weerasuriya 1984 (Weerasuriya et al., 1984) Calculation of chosen conductivity value unclear.
(Sabetian et al., 2017b)	C & D	*0.012*	25	478	Yoo 2005 (Yoo and Durand, 2005) Choi 2001 (Choi et al., 2001)
(Sabetian et al., 2017a)	C & D	*0.012*	25	478	Sabetian 2017b (Sabetian et al., 2017b)
(Raspopovic et al., 2017)	D	--	From segmentation of histology (?)	1136	Weerasuriya 1984 (Weerasuriya et al., 1984), assuming thk_{peri} = 3%*d_{fasc} and corrected from 21 to 37°C using Q_{10} = 1.5 See "Determination of Electrical Parameters: Correction of the Perineurium Conductivity" in the publication
(Pelot et al., 2017)	C	0.05	--	--	Weerasuriya 1984 (Weerasuriya et al., 1984)
(Elder and Yoo, 2018)	C & D	*0.024*	50	478	Yoo 2005 (Yoo and Durand, 2005)

Supplement B – Validation of Contact Impedance Boundary Condition

We used COMSOL's contact impedance boundary condition to model the perineurium in the 3D nerve models and to model the axon membranes in the 2D fascicle to estimate the bulk transverse endoneurial resistivity. For the former application, we compared thresholds when using a thin meshed perineurium to the perineurial boundary condition (see Figure 4 in the main text). For the latter application, we performed a simple validation of the contact impedance boundary condition used to model the axonal membranes. We compared $\rho_{endo\text{-}bulk\text{-}transverse}$ obtained by modeling the axon membrane as a physical annulus around the intracellular space (Figure 9(a)) and as a contact impedance (Figure 9(b)). To generate results within machine precision, i.e. to avoid numerical instabilities, the ratio of the model's largest to smallest resistivities must be less than six orders of magnitude. Since our model's smallest resistivity is 0.65 Ω-m (for $\rho_{endo\text{-}micro}$) and the specific membrane resistance is 0.2 Ω-m^2, we set the membrane thickness to 1 µm. Thus, the membrane resistivity was 2x10^5 Ω-m, leading to ρ_{max}/ρ_{min}=3x10^5, which is within machine precision. We placed 22 oversized axons (10 µm diameter, plus membrane thickness) in a grid within a 105 µm fascicle with 3 µm between neighbouring axons. Since our results show that no current enters the axons, we used 12 µm diameter axons when using the contact impedance in order to encompass the same area as the 10 µm axons surrounded by 1 µm thick annuli. Both models yielded $\rho_{endo\text{-}bulk\text{-}transverse}$=1.14 Ω-m (see section 2.4.2), thereby validating the boundary condition.

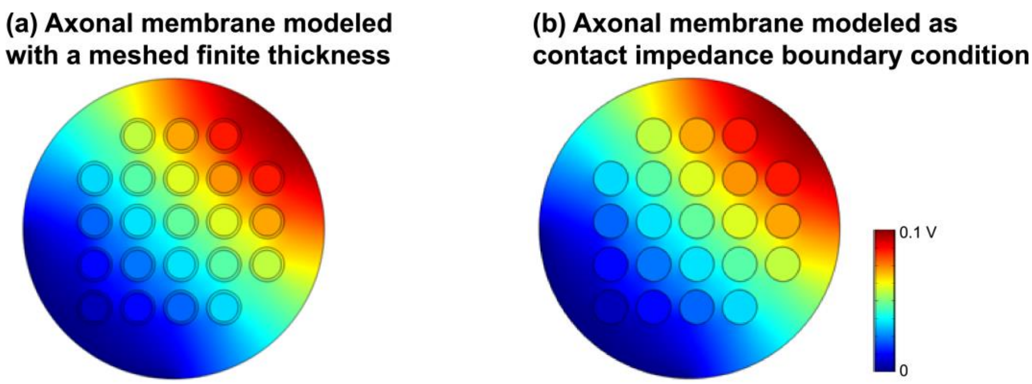

Figure 9. Potential distributions used to validate COMSOL's contact impedance boundary condition. Twenty one axons were placed in a grid within a 105 µm fascicle. We compared $\rho_{endo\text{-}bulk\text{-}transverse}$ resulting from modeling the axonal membranes as annuli with finite thickness (a) or as contact impedances (b).

Supplement C – Axonal Area Fraction Calculation

Table 5 shows calculations for estimating the axonal area fraction (*AAF*) for a single fascicle based on cat posterior abdominal vagus nerve morphology.

Table 5. Estimation of axonal area fraction in a single abdominal vagus nerve fascicle based upon cat data.

Number of fibres in cat abdominal vagus nerve (Agostini, 1957)	31,244
Total cross-sectional area of axons (Agostini, 1957; Mei et al., 1980)	$\left(\frac{31{,}244 fibers}{nerve}\right)(\pi)\left(\frac{1\mu m}{2}\right)^2 = 2.4539x10^4 \mu m^2$
Fraction of epineurium in nerve diameter (Altman and Plonsey, 1989)	0.3
Diameter of cat posterior abdominal vagus nerve (Agostini, 1957)	376 µm
Cross-sectional area of nerve, neglecting epineurium (Agostini, 1957)	$(\pi)\left(\frac{(1-0.3)*376\,\mu m}{2}\right)^2 = 5.4437x10^4\ \mu m^2$
Axonal area fraction (*AAF*)	$(2.4539 \times 10^4\ \mu m^2) / (5.4437 \times 10^4\ \mu m^2) =$ **0.45 = 45%**

Supplement D – Effects of Representation of the Perineurium on Thresholds

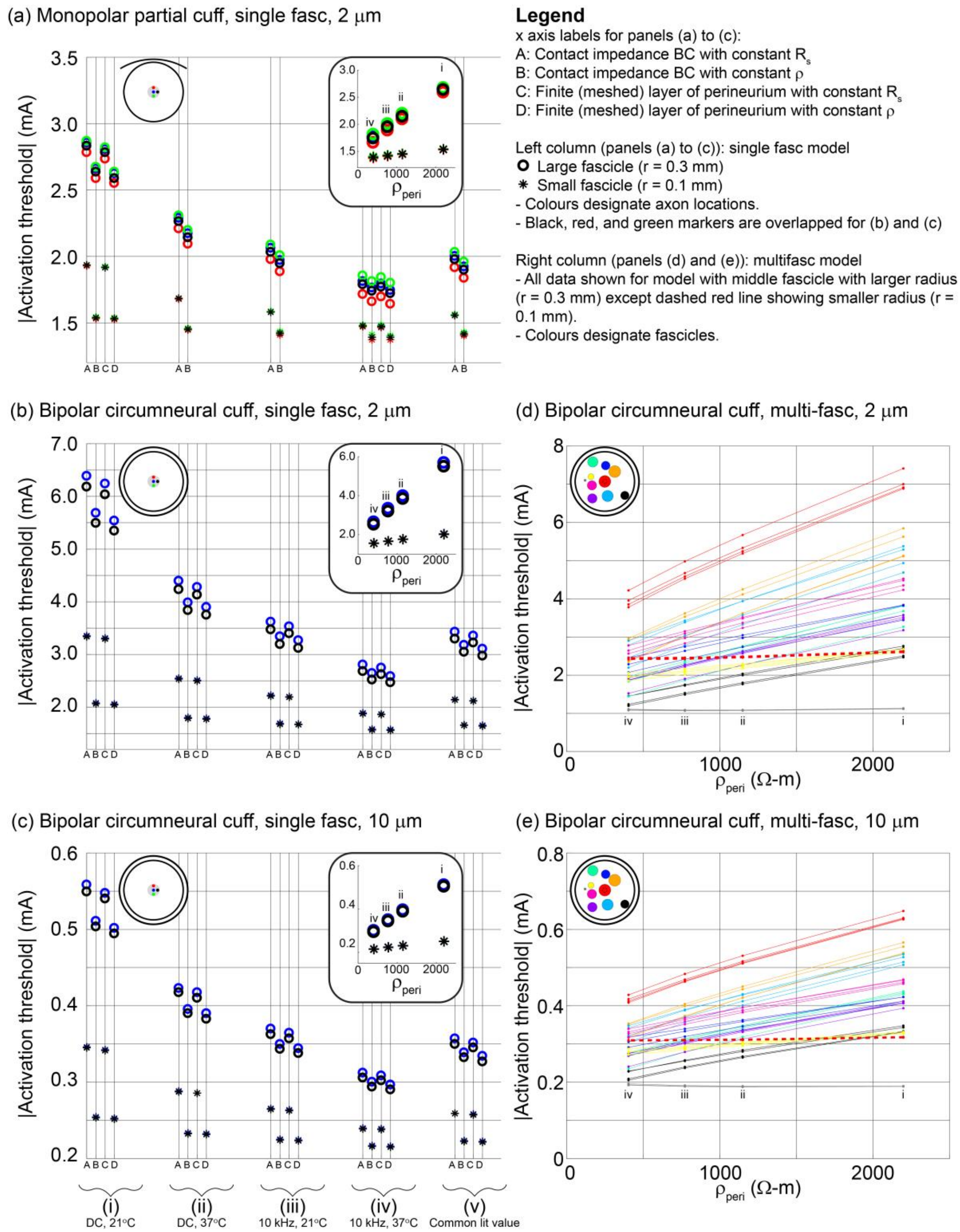

Figure 10. Activation thresholds with different representations of the perineurium (x axis labels A to D), estimates of perineurium resistivity (i to v; see Table 2), nerve models (single fascicle and multifascicular models), electrode designs (monopolar partial cuff and bipolar circumneural cuff), and fibre diameters (2 and 10 μm axons). The insets, as well as panels (d) and (e), show Method B data (constant ρ). Axon locations: centred (x_0,y_0), moved up $(x_0,y_0+0.75*r_{fasc})$, moved down $(x_0,y_0-0.75*r_{fasc})$, and translated laterally $(x_0+0.75*r_{fasc},y_0)$. In panels (b) and (c), showing activation thresholds with the bipolar circumneural cuff, the asterisks (small fascicle thresholds) for all four axon locations (different colours) are overlapped; also, given the model's symmetry, the black, red, and green circular markers (large fascicle thresholds) are overlapped. The nerve and fascicle legends are to scale.

Supplement E – Current Density in $\rho_{endo\text{-}bulk\text{-}transverse}$ Modeling

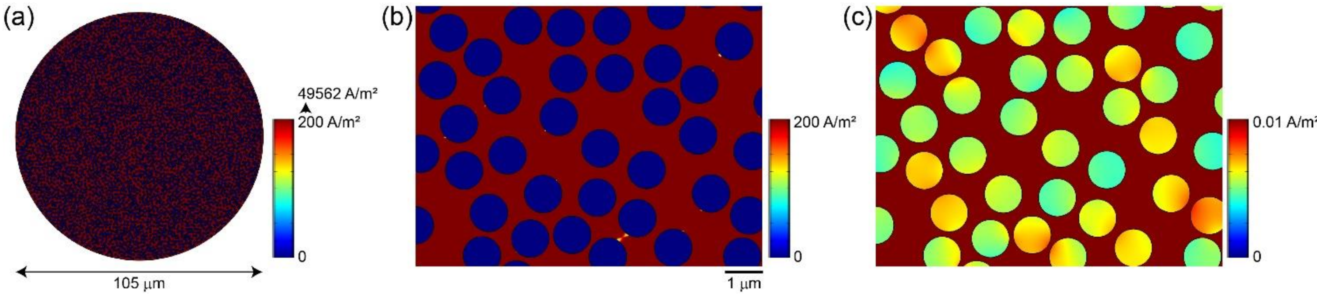

Figure 11. Magnitude of the current density showing that very little current enters the axons. Panels (b) and (c) (different colour bar bounds) are zoomed in on the centre of the entire fascicle shown in panel (a).

Supplement F – Sweeping Endoneurial Resistivity

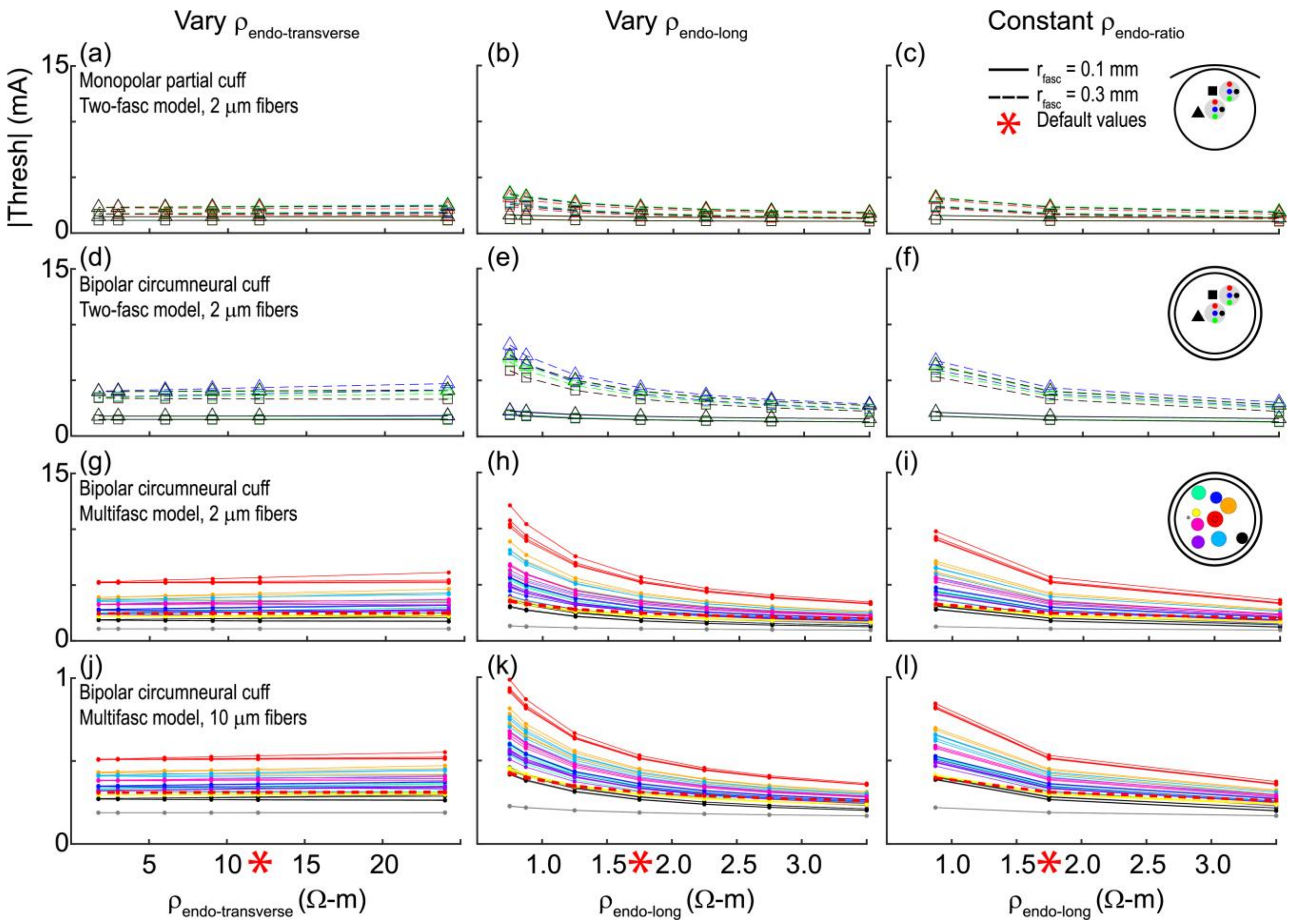

Figure 12. Activation thresholds for axons in a 3D FEM of nerve and cuff electrode across different values of endoneurial resistivity (see illustration of methods in Figure 2). The default resistivities (red asterisks) were 12 Ω-m for $\rho_{endo\text{-}transverse}$ and 1.75 Ω-m for $\rho_{endo\text{-}long}$. In the last column, the ratio of the transverse resistivity to the longitudinal resistivity was constant at 12 Ω-m/1.75 Ω-m = 6.9. All models used ρ_{peri} = 1149 Ω-m (DC, 37ºC). Similar results were found for the monopolar partial cuff with ρ_{peri} = 2198 Ω-m (DC, 21ºC) (data not shown). First and second rows: Thresholds for 2 µm axons for the nerve model with two fascicles for different cuff electrode geometries. The colours designate the four axon locations per fascicle, as shown in the legends in the last column (nerve cross sections not to scale). Third and fourth rows: Thresholds for 2 and 10 µm axons for the nerve model with 10 fascicles and the bipolar circumneural cuff geometry. The fascicle colours are shown in the legend in the last column (fascicles and nerve drawn to scale); the thresholds for four axons per fascicle are plotted in the same colour. The thresholds are plotted for the simulations where the centre fascicle (red) had a radius of 0.3 mm. The thresholds for axons in the centre fascicle when its radius was reduced (r = 0.1 mm; dashed black circle in the legend) are plotted with the dashed red lines; the thresholds for axons in other fascicles changed less than 4% between the models with the larger and the smaller centre fascicle.

References

Agostini, E., 1957. Functional and histological studies of the vagus nerve and its branches to the heart, lungs and abdominal viscera in the cat. J Physiol 135, 182–205.

Altman, K.W., Plonsey, R., 1989. Analysis of the longitudinal and radial resistivity measurements of the nerve trunk. Ann Biomed Eng 17, 313–324.

Choi, A.Q., Cavanaugh, J.K., Durand, D.M., 2001. Selectivity of multiple-contact nerve cuff electrodes: a simulation analysis. IEEE Trans Biomed Eng 48, 165–172. https://doi.org/10.1109/10.909637

Deurloo, K.E., Holsheimer, J., Boom, H.B., 1998. Transverse tripolar stimulation of peripheral nerve: a modelling study of spatial selectivity. Med Biol Eng Comput 36, 66–74.

Deurloo, K.E.I., Holsheimer, J., Bergveld, P., 2003. Fascicular selectivity in transverse stimulation with a nerve cuff electrode: a theoretical approach. Neuromodulation 6, 258–269. https://doi.org/10.1046/j.1525-1403.2003.03034.x

Elder, C.W., Yoo, P.B., 2018. A finite element modeling study of peripheral nerve recruitment by percutaneous tibial nerve stimulation in the human lower leg. Med Eng Phys 53, 32–38. https://doi.org/10.1016/j.medengphy.2018.01.004

Frieswijk, T.A., Smit, J.P., Rutten, W.L., Boom, H.B., 1998. Force-current relationships in intraneural stimulation: role of extraneural medium and motor fibre clustering. Med Biol Eng Comput 36, 422–430.

Goodall, E.V., Kosterman, L.M., Holsheimer, J., Struijk, J.J., 1995. Modeling study of activation and propagation delays during stimulation of peripheral nerve fibers with a tripolar cuff electrode. IEEE Transactions on Rehabilitation Engineering 3, 272–282. https://doi.org/10.1109/86.413200

Grinberg, Y., Schiefer, M.A., Tyler, D.J., Gustafson, K.J., 2008. Fascicular perineurium thickness, size, and position affect model predictions of neural excitation. IEEE T. Neur. Sys. Reh. 16, 572–581. https://doi.org/10.1109/TNSRE.2008.2010348

Hennings, K., Arendt-Nielsen, L., Christensen, S.S., Andersen, O.K., 2005. Selective activation of small-diameter motor fibres using exponentially rising waveforms: a theoretical study. Med Biol Eng Comput 43, 493–500.

Kent, A.R., Grill, W.M., 2013. Model-based analysis and design of nerve cuff electrodes for restoring bladder function by selective stimulation of the pudendal nerve. Journal of Neural Engineering 10, 036010. https://doi.org/10.1088/1741-2560/10/3/036010

Koole, P., Holsheimer, J., Struijk, J.J., Verloop, A.J., 1997. Recruitment characteristics of nerve fascicles stimulated by a multigroove electrode. IEEE Trans Rehabil Eng 5, 40–50.

Mei, N., Condamin, M., Boyer, A., 1980. The composition of the vagus nerve of the cat. Cell Tissue Res. 209, 423–431. https://doi.org/10.1007/BF00234756

Meier, J.H., Rutten, W.L., Zoutman, A.E., Boom, H.B., Bergveld, P., 1992. Simulation of multipolar fiber selective neural stimulation using intrafascicular electrodes. IEEE Trans Biomed Eng 39, 122–134. https://doi.org/10.1109/10.121643

Pelot, N.A., Behrend, C., Grill, W., 2017. Modeling the response of small myelinated axons in a compound nerve to kilohertz frequency signals. Journal of Neural Engineering. https://doi.org/10.1088/1741-2552/aa6a5f

Perez-Orive, J., Durand, D.M., 2000. Modeling study of peripheral nerve recording selectivity. IEEE Trans Rehabil Eng 8, 320–329.

Rahal, M., Taylor, J., Donaldson, N., 2000. The effect of nerve cuff geometry on interference reduction: a study by computer modeling. IEEE Trans Biomed Eng 47, 136–138. https://doi.org/10.1109/10.817629

Raspopovic, S., Petrini, F.M., Zelechowski, M., Valle, G., 2017. Framework for the Development of Neuroprostheses: From Basic Understanding by Sciatic and Median Nerves Models to Bionic Legs and Hands. Proceedings of the IEEE 105, 34–49. https://doi.org/10.1109/JPROC.2016.2600560

Sabetian, P., Popovic, M.R., Yoo, P.B., 2017a. Optimizing the design of bipolar nerve cuff electrodes for improved recording of peripheral nerve activity. J Neural Eng 14, 036015. https://doi.org/10.1088/1741-2552/aa6407

Sabetian, P., Sadeghlo, B., Zhang, C.H., Yoo, P.B., 2017b. Characterizing the reduction of stimulation artifact noise in a tripolar nerve cuff electrode by application of a conductive shield layer. Medical Engineering & Physics 40, 39–46. https://doi.org/10.1016/j.medengphy.2016.11.010

Schiefer, M.A., Triolo, R.J., Tyler, D.J., 2008. A model of selective activation of the femoral nerve with a flat interface nerve electrode for a lower extremity neuroprosthesis. IEEE Trans Neural Syst Rehabil Eng 16, 195–204. https://doi.org/10.1109/TNSRE.2008.918425
Struijk, J.J., 1997. The extracellular potential of a myelinated nerve fiber in an unbounded medium and in nerve cuff models. Biophys. J. 72, 2457–2469. https://doi.org/10.1016/S0006-3495(97)78890-8
Sunderland, S., Bradley, K.C., 1952. The perineurium of peripheral nerves. The Anatomical Record 113, 125–141. https://doi.org/10.1002/ar.1091130202
Veltink, P.H., van Veen, B.K., Struijk, J.J., Holsheimer, J., Boom, H.B., 1989. A modeling study of nerve fascicle stimulation. IEEE Trans Biomed Eng 36, 683–692. https://doi.org/10.1109/10.32100
Vučković, A., Struijk, J.J., Rijkhoff, N.J.M., 2005. Influence of variable nerve fibre geometry on the excitation and blocking threshold. A simulation study. Med Biol Eng Comput 43, 365–374.
Weerasuriya, A., Spangler, R.A., Rapoport, S.I., Taylor, R.E., 1984. AC impedance of the perineurium of the frog sciatic nerve. Biophys. J. 46, 167–174. https://doi.org/10.1016/S0006-3495(84)84009-6
Yoo, P.B., Durand, D.M., 2005. Selective recording of the canine hypoglossal nerve using a multicontact flat interface nerve electrode. IEEE Trans Biomed Eng 52, 1461–1469. https://doi.org/10.1109/TBME.2005.851482